

Synthesis, Structure, and Reactivity of Unsolvated Triple-Decked Bent Metallocenes of Divalent Europium and Ytterbium

William J. Evans,* Matthew A. Johnston, Michael A. Greci, and Joseph W. Ziller

Department of Chemistry, University of California, Irvine, California 92697-2025

Received September 11, 1998

The europium and ytterbium complexes of formula $[(C_5Me_5)Ln]_2(\mu-\eta^8:\eta^8-C_8H_8)$ have been synthesized and structurally characterized to determine the dependence of the (ring centroid)–metal–(ring centroid) angles on the size and electron configuration of the metal. $YbI_2(THF)_2$ reacts with KC_5Me_5 and $K_2C_8H_8$ in THF to form $[(C_5Me_5)Yb(THF)]_2(\mu-\eta^8:\eta^8-C_8H_8)$, **1**, in 80% yield. **1** can be readily desolvated at 30 °C and 10^{-7} Torr to afford $[(C_5Me_5)Yb]_2(\mu-\eta^8:\eta^8-C_8H_8)$, **2**, in 80% yield. **2** crystallizes from toluene and consists of two divalent $[(C_5Me_5)Yb]^+$ moieties bridged by a $(C_8H_8)^{2-}$ unit with 159° and 161° (C_5Me_5 ring centroid)–Yb–(C_8H_8 ring centroid) angles. $[(C_5Me_5)Eu(THF)]_2(\mu-\eta^8:\eta^8-C_8H_8)$, **3**, can be desolvated at 55 °C and 10^{-7} Torr to afford $[(C_5Me_5)Eu]_2(\mu-\eta^8:\eta^8-C_8H_8)$, **4**, in 90% yield. **4** crystallizes with a molecule of toluene and has 149.3° and 148.9° (C_5Me_5 centroid)–Eu–(C_8H_8 centroid) angles. Complex **2** reacts with 1,3,5,7-cyclooctatetraene to form $(C_5Me_5)Yb(C_8H_8)$, **5**.

Introduction

For many years the unsolvated divalent lanthanide metallocene $(C_5Me_5)_2Sm^{1,2}$ has been the subject of theoretical studies which attempt to rationalize why the C_5Me_5 rings adopt a bent structure instead of the sterically more favorable linear arrangement in which the C_5Me_5 rings are parallel.³ This molecule constitutes an organometallic case of the much broader question of why some ML_2 systems are bent instead of linear.⁴

When $(C_5Me_5)_2Sm$ was first discovered, it was suggested that perhaps it was bent because it had an 18-electron configuration or because there was something special about its $4f^6$ electron configuration. These questions prompted the preparation of the 19-electron analogue, $(C_5Me_5)_2Eu$, a half-filled-shell $4f^7$ system which was also bent.² Although a variety of other unsolvated divalent metallocenes, $(C_5Me_5)_2M$ ($M = Yb, Ba, Ca, \text{ and } Sr$), were also found to be bent, examples of other classes of unsolvated (polyhapto organic anions)₂ M complexes of these divalent metals were unavailable for comparison except for the Yb(II) cyclooctatetraenyl complex, $(DME)K(C_8H_8)Yb(C_8H_8)K(DME)$, which had parallel rings.⁶

The recent discovery of the mixed ligand compound $[(C_5Me_5)Sm]_2(\mu-\eta^8:\eta^8-C_8H_8)^7$ provided an opportunity to evaluate another class of compounds in which an f-element was sandwiched between two polyhapto organic anions. It should be noted that the cyclooctatetraenide dianion and its substituted derivatives have been used to form a variety of bimetallic⁸ and trimetallic^{8c,9} multidecker lanthanide complexes. By X-ray crystallography, it was determined that $[(C_5Me_5)Sm]_2(\mu-\eta^8:\eta^8-C_8H_8)$ has a bent structure in which the (C_5Me_5 ring centroid)–Sm–(C_8H_8 ring centroid) angles were 149.3° and 148.9°; that is, this C_5Me_5/C_8H_8 complex followed the pattern of C_5Me_5 , not C_8H_8 f element metallocenes. As in the $(C_5Me_5)_2Sm$ case, it was of interest to determine if the europium and ytterbium analogues of $[(C_5Me_5)Sm]_2(\mu-\eta^8:\eta^8-C_8H_8)$ could be made and if crystals suitable for X-ray diffraction could be obtained, so that the effects of electron configuration and radial size could be evaluated in this triple-decked metallocene system.

We report here the synthesis and structure of the europium and ytterbium analogues of $[(C_5Me_5)Sm]_2(\mu-\eta^8:\eta^8-C_8H_8)$, as well as some preliminary reactivity studies. Since the most desirable europium precursor, $[(C_5Me_5)Eu(THF)]_2(\mu-\eta^8:\eta^8-C_8H_8)^{10}$ had already been made and structurally characterized, formation of the desolvated europium complex could be attempted from a known starting material. In the case of ytterbium, a synthesis of the solvated precursor, $[(C_5Me_5)Yb(THF)]_2(\mu-\eta^8:\eta^8-C_8H_8)$, was first needed, and this is also reported here.

(1) Evans, W. J.; Hughes, L. A.; Hanusa, T. P. *J. Am. Chem. Soc.* **1984**, *106*, 4270.

(2) Evans, W. J.; Hughes, L. A.; Hanusa, T. P. *Organometallics* **1986**, *5*, 1285.

(3) (a) Ortiz, J. V.; Hoffman, R. *Inorg. Chem.* **1985**, *24*, 2095. (b) Kaupp, M.; Schleyer, P. v. R.; Dolg, M.; Stoll, H. *J. Am. Chem. Soc.* **1992**, *114*, 8202. (c) Hollis, T. K.; Burdett, J. K.; Bosnich, B. *Organometallics* **1993**, *12*, 3385. (d) Bosnich, B. *Chem. Soc. Rev.* **1994**, 387. (e) Bordreaux, E. A.; Baxter, E. *Int. J. Quantum Chem.: Quantum Chem. Symp.* **1994**, *28*, 565. (f) Timofeeva, T. V.; Lii, J.-H.; Allinger, N. L. *J. Am. Chem. Soc.* **1995**, *117*, 7452.

(4) The extensive literature on this point is documented in: Kaupp, M.; Schleyer, P. v. R.; Stoll, H.; Preuss, H. *J. Am. Chem. Soc.* **1991**, *113*, 6012.

(5) (a) Williams, R. A.; Hanusa, T. P.; Huffman, J. C. *Organometallics* **1990**, *9*, 1128. (b) Tilley, T. D.; Andersen, R. A.; Zalkin, A. *J. Am. Chem. Soc.* **1982**, *104*, 3725. (c) Andersen, R. A.; Blom, R.; Burns, C. J.; Volden, H. V. *J. Chem. Soc., Chem. Commun.* **1987**, 768.

(6) Boussie, T. R.; Eisenberg, D. C.; Rigsbee, J.; Streitweiser, A.; Zalkin, A. *Organometallics* **1991**, *10*, 1922.

(7) Evans, W. J.; Clark, R. D.; Ansari, M. A.; Ziller, J. W. *J. Am. Chem. Soc.* **1998**, *120*, 9555.

(8) (a) Greco, A.; Cesca, S.; Bertolini, G. *J. Organomet. Chem.* **1976**, *11*, 171. (b) DeKock, C. W.; Ely, S. R.; Hopkins, T. E.; Brault, M. A. *Inorg. Chem.* **1978**, *17*, 625. (c) Edelmann, F. T. *New. J. Chem.* **1995**, *19*, 535.

(9) Fisher, R. D. *Angew. Chem., Int. Ed. Engl.* **1994**, *33*, 2166.

Experimental Section

All manipulations involving $[(C_5Me_5)Ln]_2(\mu-\eta^8-\eta^8-C_8H_8)$ and its reaction products were carried out under argon in an inert atmosphere glovebox free of coordinating solvents. All other chemistry was performed under nitrogen with rigorous exclusion of air and water by using Schlenk, vacuum line, and glovebox techniques. Physical measurements were obtained and solvents were purified as previously described.¹¹ $YbI_2 \cdot (THF)_2$ ¹² and $[(C_5Me_5)Eu(THF)_2]_2(\mu-\eta^8-\eta^8-C_8H_8)$ ¹⁰ were prepared following literature procedures. 1,3,5,7-Cyclooctatetraene (Aldrich) was dried over activated 4A molecular sieves and was vacuum distilled before use. $K_2C_8H_8$ was prepared from potassium and 1,3,5,7-cyclooctatetraene according to literature procedures.¹³ 1H and ^{13}C NMR spectra were obtained using Omega 500 MHz and Bruker DRX-400 MHz NMR spectrometers at 25 °C. IR spectra were obtained using a Perkin-Elmer series 1600 FTIR spectrophotometer, and UV-vis spectra were obtained using a Shimadzu 160 spectrophotometer. Complexometric analyses for Eu and Yb were performed as previously described.¹⁴ C and H analyses were performed by Desert Analytics, Tucson, AZ, 85719.

$[(C_5Me_5)Yb(THF)]_2(C_8H_8)$, 1. $YbI_2(THF)_2$ (5.00 g, 8.7 mmol) and KC_5Me_5 (1.53 g, 8.7 mmol) were stirred in 8 mL of THF and formed a cloudy purple suspension. To this mixture, a solution of $K_2C_8H_8$ (0.80 g, 4.4 mmol) in THF was added dropwise, causing the color to change to deep brown. After 4 h of stirring, the reaction was centrifuged to remove white insoluble material. THF was removed from the red-brown supernatant by rotary evaporation, leaving **1** as a red-brown powder (3.15 g, 81%). 1H NMR (C_6D_6 , 20 °C): δ 5.76 (s, 8H, C_8H_8), 3.28 (m, 8H, THF), 1.79 (s, 30H, C_5Me_5), 1.35 (m, 8H, THF). $^{13}C\{^1H\}$ NMR (C_6D_6 , 20 °C): δ 111.74 (C_5Me_5), 89.52 (C_8H_8), 67.13 (THF), 25.60 (THF), 10.43 (C_5Me_5). UV-vis (hexane): λ_{max} 639, 536, 425 nm. FTIR (KBr): 2908 s, 2850 w, 1725 m, 1614 w, 1437 m, 1261 w, 1091 m, 1020 m, 797 w, 720 cm^{-1} . Anal. Calcd for $Yb_2C_{36}H_{54}O_2$: Yb, 40.0. Found: Yb, 39.9.

$[(C_5Me_5)Yb]_2(C_8H_8)$, 2. In a tube fitted with a high-vacuum stopcock, **1** (3.15 g, 3.6 mmol) was heated to 30 °C at 10^{-7} Torr on a vacuum line. The color changed from a red-brown to bright green within 3 h. The material was brought into a THF-free glovebox and extracted with 10 mL of toluene. Removal of toluene afforded **2** (2.20 g, 83%) as a bright green powder. 1H NMR (C_6D_6 , 20 °C): δ 5.703 (s, 8H, C_8H_8), 1.731 (s, 30H, C_5Me_5). $^{13}C\{^1H\}$ NMR (C_6D_6 , 20 °C): δ 112.20 (C_5Me_5), 90.31 (C_8H_8), 10.10 (C_5Me_5). Variable-temperature NMR (C_7D_8 , -80 °C): No change observed in the peak pattern. UV-vis (hexane): λ_{max} 648, 419 nm. FTIR (KBr): 2899 s, 1739 s, 1451 w, 1387 w, 1099 m, 1017 m, 887 w cm^{-1} . Anal. Calcd for $Yb_2C_{28}H_{38}$: Yb, 48.0; C, 46.66; H, 5.31. Found: Yb, 47.4; C, 47.16; H, 5.30. Mp > 300 °C. Recrystallization of **2** from toluene at -35 °C provided crystals suitable for X-ray analysis.

X-ray Data Collection, Structure Determination, and Refinement for 2. A green crystal of the approximate dimensions $0.46 \times 0.43 \times 0.10$ mm was mounted on a glass fiber and transferred to a Siemens P4 diffractometer. The determination of symmetry, crystal class, unit cell parameters, and the crystal's orientation matrix was carried out according to standard procedures.¹⁵ Intensity data were collected at 163 K using $2\theta/\omega$ scan technique with Mo K α radiation. The raw data were processed with a local version of CARESS¹⁶ which

employs a modified version of the Lehman-Larsen algorithm to obtain intensities and standard deviations from the measured 96-step peak profiles. Subsequent calculations were carried out using the SHELXTL program.¹⁷ All 11 704 data were corrected for absorption and for Lorentz and polarization effects and were placed on an approximately absolute scale. There were no systematic absences nor any diffraction symmetry other than the Friedel condition. The centrosymmetric space group $P\bar{1}$ was assigned and later determined to be correct.

The structure was solved by direct methods and refined on F^2 by full-matrix least-squares techniques. The analytical scattering factors for neutral atoms were used throughout the analysis.¹⁸ Hydrogen atoms were included using a riding model. At convergence, $wR2 = 0.1777$ and $GOF = 1.032$ for 542 variables refined against all 11 224 unique data. (As a comparison for refinement on F , $R1 = 0.0604$ for those 8750 data with $F > 4.0\sigma(F)$.)

$[(C_5Me_5)Eu]_2(C_8H_8) \cdot C_7H_8$, 4. As described for **2**, $[(C_5Me_5)Eu(THF)_2]_2(C_8H_8)$,¹⁰ **3** (4.5 g, 4.6 mmol), was heated at 50 °C and 10^{-7} Torr and changed from a deep orange-brown to a bright orange. The material was extracted with 15 mL of toluene in a THF-free glovebox. Removal of solvent afforded **4** as a bright orange powder (2.9 g, 92%). UV-vis (hexane): λ_{max} 440, 394 nm. FTIR (KBr): 2964 s, 2882 w, 1733 w, 1718 w, 1620 s, 1461 m, 1256 m, 1159 w, 1025 m. Anal. Calcd for $Eu_2C_{28}H_{38}$: Eu, 44.8; C, 49.56; H, 5.64. Found: Eu, 44.6; C, 49.54; H, 5.72. Mp > 300 °C. Recrystallization of **4** from toluene at -35 °C provided crystals suitable for X-ray analysis.

X-ray Data Collection, Structure Determination, and Refinement for 4. The structural analysis of **4** followed the procedures used for **2** unless otherwise noted. An orange crystal of the approximate dimensions $0.23 \times 0.16 \times 0.10$ mm was mounted on a glass fiber and transferred to a Siemens P4 diffractometer. Intensity data was collected at 153 K. All 3456 data were corrected for absorption, Lorentz, and polarization effects and were placed on an approximately absolute scale. The diffraction symmetry was mmm with systematic absences $h = 2n+1$ for $h00$, $k = 2n+1$, for $0k0$, and $l = 2n+1$ for $00l$. The noncentrosymmetric orthorhombic space group $P2_12_12_1$ [D^4_2 ; No. 19] is therefore uniquely defined.

Refinement of the Flack parameter was inconclusive in determining the absolute structure. The structure was refined as a racemic twin using the TWIN parameter in SHELXTL. One molecule of toluene per bimetallic complex was located. At convergence, $wR2 = 0.1665$ and $GOF = 1.255$ for 347 variables refined against all 3456 unique data. (As a comparison for refinement on F , $R1 = 0.0526$ for those 2762 data with $F > 4.0\sigma(F)$.)

$(C_5Me_5)Yb(C_8H_8)$, 5. 1,3,5,7-Cyclooctatetraene (0.011 g, 0.11 mmol) was added by syringe to a stirred solution of **2** (0.078 g, 0.11 mmol) in 5 mL of toluene, and the reaction mixture immediately changed from green to purple. Removal of solvent by rotary evaporation gave **5** as a purple microcrystalline solid (0.084 g, 93%). 1H NMR (C_6D_6 , 20 °C): δ 5.8 (broad s, 15H) -14.9 (broad s, 8H). $^{13}C\{^1H\}$ NMR (C_6D_6 , 20 °C): δ 117.84 (C_5Me_5), 79.86 (C_8H_8), 20.10 (C_5Me_5). UV-vis (hexane): λ_{max} 720, 552. FTIR (KBr): 3030 w, 2866 s, 1745 w, 1592 w, 1445 m, 1381 m, 1263 s, 1093 s, 1028 s, 893 m, 799 m cm^{-1} . Anal. Calcd for $YbC_{18}H_{23}$: Yb, 41.95; C, 52.42; H, 5.57. Found: Yb, 41.5; C, 52.04; H, 5.78. Mp: 246-248 °C. Recrystallization from toluene at -35 °C provided crystals suitable for X-ray structure analysis. The unit cell parameters showed that **5** is isomorphous with $(C_5Me_5)Lu(C_8H_8)$:¹⁹ space group $Pnam$, $a = 10.300(3)$ Å, $b = 11.585(2)$ Å, $c = 12.997(2)$ Å, and $V = 1550.98(71)$ Å³.

(10) Evans, W. J.; Shreeve, J. L.; Ziller, J. W. *Polyhedron* **1995**, *14*, 2945.

(11) (a) Evans, W. J.; Chamberlain, L. R.; Ulibarri, T. A.; Ziller, J. W. *J. Am. Chem. Soc.* **1985**, *107*, 1671. (b) Evans, W. J.; Chamberlain, L. R.; Ulibarri, T. A.; Ziller, J. W. *J. Am. Chem. Soc.* **1988**, *110*, 6423.

(12) Namy, J. L.; Girard, P.; Kagan, H. B. *New. J. Chem.* **1977**, *1*, 5.

(13) Wayda, A. L. In *Inorganic Syntheses*; Ginsberg, A. P., Ed.; Wiley: New York, 1990; Vol. 27, p 150.

(14) Evans, W. J.; Ergerer, S. C.; Coleson, K. M. *J. Am. Chem. Soc.* **1981**, *103*, 6672.

(15) *XSCANS Software Users Guide*, Version 2.1; Siemens Industrial Automation, Inc.: Madison, WI, 1994.

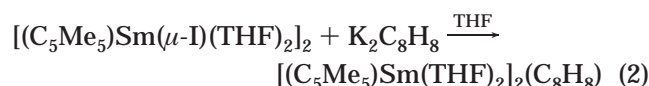
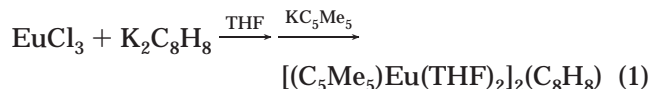
(16) Broach, R. W. *CARESS*; Argonne National Laboratory: Illinois, 1978.

(17) Sheldrick, G. M. *SHELXTL*; Siemens Analytical X-ray Instruments, Inc.: Madison, WI, 1994.

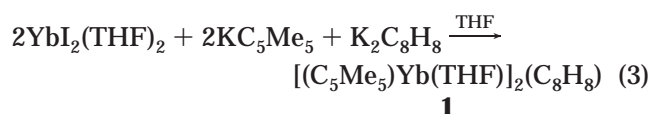
(18) *International Tables for X-ray Crystallography*; Kluwer Academic Publishers: Dordrecht, The Netherlands, 1992; Vol. C.

Results

Synthesis of Solvated $[(C_5Me_5)Yb(THF)]_2(\mu-\eta^8:\eta^8-C_8H_8)$, **1.** The synthesis of the ytterbium analogue of the solvated $[(C_5Me_5)Ln(THF)]_2(C_8H_8)$ complexes known for $Ln = Sm$ and Eu could not be accomplished by the synthetic routes shown in eqs 1 and 2 for these reasons: (a) $Yb(III)$ is not reduced like $Eu(III)$ in eq 1



and (b) the precursor needed for a reaction analogous to eq 2, $[(C_5Me_5)Yb(\mu-I)(THF)_2]_2$, was not known when this research was undertaken. Fortunately, the equivalent of the latter complex can be generated in situ, and direct reaction of $YbI_2(THF)_2$, KC_5Me_5 , and $K_2C_8H_8$ in THF results in the formation of $[(C_5Me_5)Yb(THF)]_2-(C_8H_8)$, **1**, in good yield, as shown in eq 3. After the

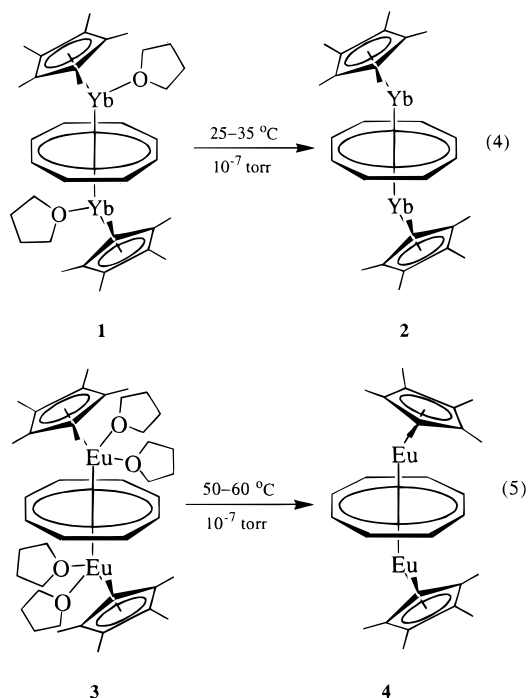


development of the synthesis in eq 3, the synthesis of $[(C_5Me_5)Yb(\mu-I)(THF)_2]_2$ was reported in the literature.²⁰ However, the reaction of $[(C_5Me_5)Yb(\mu-I)(THF)_2]_2$ with $K_2C_8H_8$ repeatedly afforded poorer yields of **1** than the one-step synthesis shown in eq 3.

Compound **1** was characterized by elemental analysis and IR and NMR spectroscopy. The infrared spectra of **1** and $[(C_5Me_5)Eu(THF)_2]_2(C_8H_8)$ are nearly identical. In THF, **1** forms a red-brown solution. The NMR spectra of **1** are consistent with the presence of divalent, diamagnetic ytterbium. The C_8H_8 resonance is located at 5.76 ppm, the C_5Me_5 resonance is at 1.79 ppm, and these signals integrate 8:30 as expected. The ^{13}C NMR spectrum exhibits three peaks at 111.74, 89.52, and 10.43, corresponding to the C_5Me_5 , C_8H_8 , and C_5Me_5 carbons, respectively. Signals consistent with one THF molecule per ytterbium are also observed.

Desolvation of $[(C_5Me_5)Ln(THF)_2(\mu-\eta^8:\eta^8-C_8H_8)]$. Both $[(C_5Me_5)Yb(THF)]_2(C_8H_8)$ and $[(C_5Me_5)Eu(THF)]_2-(C_8H_8)$ desolvate (eqs 4 and 5) under conditions much milder than those observed for the desolvation of the $(C_5Me_5)_2Ln(THF)_n$ metallocenes for Eu^2 and Yb ,⁵ which require 75–80 °C and 10^{-5} – 10^{-7} Torr.

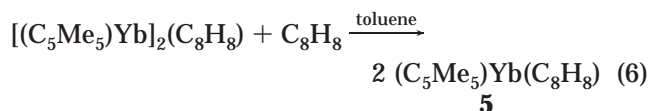
The infrared spectra of **2** and **4** exhibit similar peaks. The 1H NMR spectrum of **2** reveals signals slightly shifted from those of **1**: the C_8H_8 ring resonance is at 5.70 ppm, and the C_5Me_5 resonance is at 1.71 ppm. The THF signals are no longer present. Both **2** and **4** crystallize readily from concentrated toluene solutions at –35 °C, and the orientation of their rings could be determined by X-ray crystallography.



Structures of $[(C_5Me_5)Ln]_2(\mu-\eta^8:\eta^8-C_8H_8)$ Complexes. The structures of **2** and **4** are shown in Figures 1 and 2, and a comparative summary of bond distances and angles between **2**, **4**, and $[(C_5Me_5)Sm]_2(\mu-\eta^8:\eta^8-C_8H_8)$, **6**, is given in Table 2. The $M-C(C_5Me_5)$ bond lengths in **4** and **6** are identical within experimental error, 2.79(3) and 2.79(1) Å, respectively, as is expected since Eu and Sm differ in size by only 0.02 Å.²¹ These distances are also the same as the 2.79(1) Å average $M-C(C_5Me_5)$ distances in $(C_5Me_5)_2Eu$ and $(C_5Me_5)_2Sm$. The 2.63(2) Å $Yb-C(C_5Me_5)$ bond distance in **2** is shorter since $Yb(II)$ is 0.13 Å smaller than $Sm(II)$.²¹

Like **6**, both **2** and **4** adopt a bent rather than parallel arrangement of the rings. The 147.2° and 149.5° (C_5Me_5 centroid)– Ln –(C_8H_8 centroid) angles in **4** are very similar to those in **6**, 149.3° and 148.9°. The analogous angles in **2**, 161.2° and 159.5°, are significantly larger. For comparison, the (C_5Me_5 centroid)– Ln –(C_5Me_5 centroid) angles are 140.3° in $(C_5Me_5)_2Eu$, 140.1° in $(C_5Me_5)_2Sm$,²² and 145.7° and 145.0° in $(C_5Me_5)_2Yb$.²³ A cis arrangement of the C_5Me_5 rings is found in **4** compared to a trans arrangement in **2** and **6**, although the closest intermolecular $Eu\cdots CH_3$ distance in **4**, 3.3 Å, is similar to the 3.25 Å distance in **6**.⁷ Complex **4** does differ in that it contains a molecule of cocrystallized toluene.

Reactivity. Reaction of **2** with 1 equiv of C_8H_8 instantaneously afforded $(C_5Me_5)Yb(C_8H_8)$, **5**, as a purple solid, eq 6. This reaction is analogous to the reaction of



6 with C_8H_8 . This reaction formally constitutes a two-electron oxidative addition of C_8H_8 to a $(C_5Me_5)Yb$ unit, although the reaction does not involve an $Yb(I)/Yb(III)$

(19) Schumann, H.; Kohn, R. D.; Reier, F. W.; Dietrich, A.; Pickardt, J. *Organometallics* **1989**, 8, 1388.

(20) Constantine, S. P.; DeLima, G. M.; Hitchcock, P. B.; Keates, J. M.; Lawless, G. A. *Chem. Commun.* **1996**, 2421.

(21) Shannon, R. D. *Acta Crystallogr.* **1976**, A32, 751.

(22) Evans, W. J.; Hughes, L. A.; Hanusa, T. P. *Organometallics* **1986**, 5, 1285.

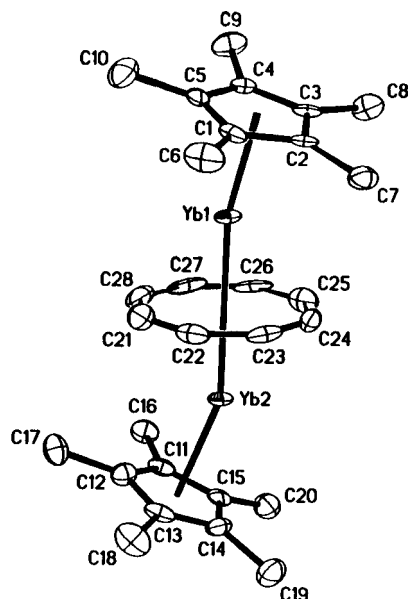


Figure 1. Thermal ellipsoid plot for $[(C_5Me_5)Yb]_2(\mu-\eta^8:\eta^8-C_8H_8)$, **2**. Thermal ellipsoids are drawn at 50% probability.

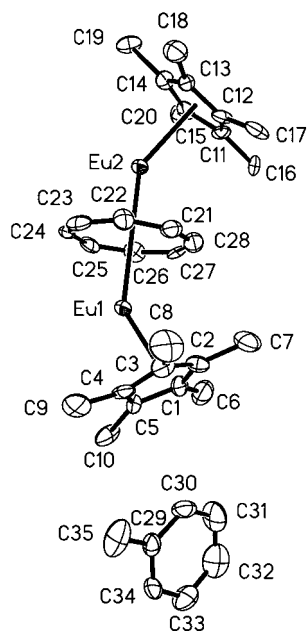


Figure 2. Thermal ellipsoid plot for $[(C_5Me_5)Eu]_2(\mu-\eta^8:\eta^8-C_8H_8) \cdot C_7H_8$, **4**. Thermal ellipsoids are drawn at 50% probability.

redox couple since the starting material has both ytterbium atoms in the +2 oxidation state.

Discussion

The synthetic results described here show that convenient routes to triple-decked mixed ligand C_5Me_5/C_8H_8 complexes are available for divalent ytterbium and europium as well as samarium.⁷ Desolvation of the solvated triple-decked complexes is considerably more facile than desolvation of the $(C_5Me_5)_2Ln(THF)_x$ complexes,²⁴ and hence the $[(C_5Me_5)Ln]_2(\mu-\eta^8:\eta^8-C_8H_8)$ com-

Table 1. Experimental Data for the X-ray Diffraction Studies of $[(C_5Me_5)Yb]_2(\mu-\eta^8:\eta^8-C_8H_8)$, **2, and $[(C_5Me_5)Eu]_2(\mu-\eta^8:\eta^8-C_8H_8)$, **4****

	2	4
formula	$Yb_2C_{28}H_{38}$	$Eu_2C_{35}H_{46}$
fw	720.69	770.64
temp (K)	163	153
cryst syst	triclinic	orthorhombic
space group	$P\bar{1}$	$P2_12_12_1$
<i>a</i> (Å)	13.338(2)	11.856(6)
<i>b</i> (Å)	13.549(2)	15.220(6)
<i>c</i> (Å)	15.815(2)	17.399(6)
α (deg)	114.772(7)	90
β (deg)	93.948(11)	90
γ (deg)	90.803(14)	90
<i>V</i> (Å ³)	2585.9(7)	3139.9(23)
<i>Z</i>	4	4
ρ_{calcd} (Mg/m ³)	1.851	1.630
diffractometer ^a	Siemens P4	Siemens P4
μ (mm ⁻¹)	7.200	3.979
<i>R</i> [$I > 2\sigma(I)$] ^b	0.0604	0.0526
<i>wR</i> ² ^b	0.1607	0.1665

^a Radiation: Mo K α ($\mu = 0.710\ 73\ \text{\AA}$). Monochromator: highly oriented graphite. ^b $R = \sum ||F_o| - |F_c|| / \sum |F_o|$; $wR^2 = [\sum (w(F_o^2 - F_c^2))^2 / \sum w(F_o^2)]^{1/2}$.

plexes are synthetically attractive when a bent lanthanide metallocene is needed.

The synthesis and crystallographic characterization of desolvated $[(C_5Me_5)Ln]_2(\mu-\eta^8:\eta^8-C_8H_8)$ complexes for the three most readily available divalent lanthanides allow a comparison of the $(C_5Me_5 \text{ centroid})-Ln-(C_8H_8 \text{ centroid})$ angles as a function of metal radius, as has been done with the unsolvated $(C_5Me_5)_2M$ complexes with a variety of metals by Hanusa et al.^{23a} The data assembled by Hanusa along with the data for **2**, **4**, and **6** are presented in Figure 3. Although only three examples are known so far for the $[(C_5Me_5)Ln]_2(\mu-\eta^8:\eta^8-C_8H_8)$ series, they show the same trend in bending as was found for the $(C_5Me_5)_2M$ complexes, namely, that a larger angle, i.e., a greater tendency toward parallel planes, is found with the smaller metals. This trend also matches the correlation found in gas-phase structures of MX_2 complexes, namely, that the larger more polarizable metals have larger X–M–X angles. These data show that theoretical explanations for the bent structures of these metallocenes must include unsubstituted C_8H_8 ligands as well as C_5Me_5 groups. Attractive $Me \cdots Me$ interactions cannot be used to explain the data presented here.²⁵

The reduction of cyclooctatetraene indicates that **2** has a reduction potential of at least $-1.83\ \text{V}$ (vs SCE), the measured potential for $(C_8H_8)/(C_8H_8)^{2-}$ reduction.²⁶ This is larger than is usually expected for Yb(II) complexes, and attempts to better define this reduction chemistry are under way. The europium complex **4** is much less reactive than the ytterbium complex **2**, as is

(23) (a) Burkey, D. J.; Hanusa, T. P. *Comments Inorg. Chem.* **1995**, 17, 41. (b) Burns, C. J. Ph.D. Thesis, University of California, Berkeley, 1987.

(24) Berg, D. J.; Burns, C. J.; Andersen, R. A.; Zalkin, A. *Organometallics* **1989**, 8, 1865.

(25) A referee has correctly pointed out that although H(methyl) \cdots H(methyl) interactions cannot be used to explain the bent structure in these molecules, one could consider H(methyl) \cdots H(cyclooctatetraenyl) interactions. However, if that were the case, one might expect the tetramethylethyl complex, $[(C_5Me_4Et)Sm]_2(C_8H_8)$, would have a more bent angle and would have the ethyl groups oriented to interact with the C_8H_8 ring. In fact, the inter-ring angle is larger and the ethyl groups are at the open part of the wedge furthest from the C_8H_8 ring hydrogens.

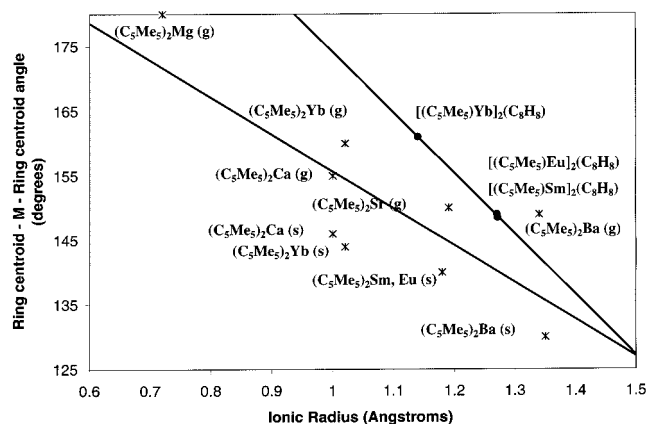
(26) Evans, W. J.; Gonzales, S. L.; Ziller, J. W. *J. Am. Chem. Soc.* **1994**, 116, 2600.

Table 2. Selected Bond Lengths (Å) and Angles (deg) for $[(C_5Me_5)Yb]_2(\mu-\eta^8:\eta^8-C_8H_8)$, **2**, $[(C_5Me_5)Eu]_2(\mu-\eta^8:\eta^8-C_8H_8)$, **4**, and $[(C_5Me_5)Sm]_2(\mu-\eta^8:\eta^8-C_8H_8)$, **6**

2		4	
atoms	distance/angle	atoms	distance/angle
Yb(1)–Cnt(1) ^a	1.909	Eu(1)–Cnt(1) ^a	2.129
Yb(2)–Cnt(1) ^a	1.926	Eu(2)–Cnt(1) ^a	2.166
Yb(1)–Cnt(2) ^b	2.338	Eu(1)–Cnt(2) ^b	2.506
Yb(2)–Cnt(3) ^c	2.346	Eu(2)–Cnt(3) ^c	2.532
Yb(1)–C(1–5) ^f	2.632(6)	Eu(1)–C(1–5) ^f	2.77(1)
Yb(2)–C(11–15)	2.636(2)	Eu(2)–C(11–15)	2.81(1)
Yb(1)–C(21–28)	2.652(2)	Eu(1)–C(21–28)	2.81(1)
Yb(2)–C(21–28)	2.665(3)	Eu(2)–C(21–28)	2.83(1)
Cnt(2) ^b –Yb(1)–Cnt(1) ^a	161.2	Cnt(2) ^b –Eu(1)–Cnt(1) ^a	147.2
Cnt(3) ^c –Yb(2)–Cnt(1) ^a	159.2	Cnt(3) ^c –Eu(2)–Cnt(1) ^a	149.5

6		6	
atoms	distance/angle	atoms	distance/angle
Sm(1)–Cnt(1) ^d	2.510	Sm(2)–C(11–15) ^f	2.77(1)
Sm(1)–Cnt(2) ^e	2.151	Sm(1)–C(21–28b) ^g	2.84(3)
Sm(2)–Cnt(2) ^e	2.120	Sm(2)–C(21–28b) ^g	2.81(3)
Sm(2)–Cnt(3) ^c	2.497	Cnt(1) ^d –Sm(1)–Cnt(2) ^e	149.3
Sm(1)–C(1–5) ^f	2.79(1)	Cnt(2) ^e –Sm(2)–Cnt(3) ^c	148.9

^a Cnt(1) is the centroid of the C(21)–C(28) ring. ^b Cnt(2) is the centroid of the C(1)–C(5) ring. ^c Cnt(3) is the centroid of the C(11)–C(15) ring. ^d Cnt(1) is the centroid of the C(1)–C(5) ring. ^e Cnt(2) is the centroid of the C(21)–C(28) ring. ^f Average of the Ln–C(ring) distances. ^g Average of the Sm–C(ring) distances for both partially occupied rings, C(21)–C(28) and C(21b)–C(28b).

**Figure 3.** Comparative plot of ionic radii versus (ring centroid)–metal–(ring centroid) angles for $(C_5Me_5)_2M$ and $[(C_5Me_5)Ln]_2(C_8H_8)$ systems.

consistent with the much weaker reduction potential of Eu(II).

Conclusion

The triple-decked mixed ligand metallocenes, $[(C_5Me_5)Ln]_2(\mu-\eta^8:\eta^8-C_8H_8)$, are synthetically accessible for Ln = Eu and Yb as well as from Sm and constitute a new series of unsolvated sterically unsaturated organolanthanide complexes. The complexes are bent regardless of the $4f^6$, $4f^7$, and $4f^{14}$ electron configurations, and the amount of bending depends on the radius of the metal as was noted earlier for the $(C_5Me_5)_2Ln$ metallocenes. The reduction of C_8H_8 by $[(C_5Me_5)Yb]_2(\mu-\eta^8:\eta^8-C_8H_8)$ indicates that it has a substantial reduction chemistry like that of $[(C_5Me_5)Sm]_2(\mu-\eta^8:\eta^8-C_8H_8)$.

Supporting Information Available: Crystal data for **2** and **4**. This material is available free of charge via the Internet at <http://pubs.acs.org>.

OM980762R